ELSEVIER

Polymer 42 (2001) 8499–8510

polymer

www.elsevier.com/locate/polymer

# Synthesis in microemulsion and characterization of stimuli-responsive polyelectrolytes and polyampholytes based on *N*-isopropylacrylamide

O. Braun, J. Selb, F. Candau*

*Institut Charles Sadron, 6 rue Boussingault, 67083 Strasbourg Cedex, France*

Received 19 April 2001; received in revised form 8 June 2001; accepted 11 June 2001

**Abstract**

Series of stimuli-responsive polyelectrolytes and polyampholytes based on *N*-isopropylacrylamide (NIPAM) have been synthesized by a microemulsion polymerization technique. The formulation of the polymerizable microemulsions was optimized by using cohesive energy ratio (CER) and hydrophile-lipophile balance (HLB) concepts, with special emphasis given to the role of the monomers. Moreover, a semi-continuous process was developed which allowed us to significantly reduce the surfactant level needed for the formulation of the microemulsion. The nucleation mechanism was investigated by dynamic light scattering experiments through the evolution of the particle size with the extent of polymerization. The final inverse latexes are clear and stable, of low particle size ($d \sim 70$ nm) and contain up to 20 wt% of high molecular weight NIPAM-based charged polymers. Under the experimental conditions selected, the latter samples are shown to be homogeneous in composition, irrespective of the monomer feed composition. 

*Keywords*: Poly(*N*-isopropylacrylamide); Poly(Sodium 2-acrylamido-2-methylpropanesulfonate); Poly(2-acrylamido-2-propanetrimethylammonium chloride)

## 1. Introduction

In the past years, there has been considerable interest in the use of materials that are stimuli-responsive, i.e. whose properties can be varied by tuning external parameters such as temperature [1,2], pH [3,4], ionic strength [5], electric field [6,7] or shear rate [8,9]. In this respect poly(*N*-isopropylacrylamide) (PNIPAM) which exhibits a well-defined lower critical solution temperature (LCST) in water around 32°C is one of the most studied temperature-responsive polymers [10–20]. Also of particular interest are materials, which respond to several stimuli either simultaneously or independently (e.g. pH, ionic strength and temperature). These materials can be obtained for example by copolymerization of NIPAM with an ionic monomer [20–24] or by grafting PNIPAM side chains on an ionized polymeric backbone [25–27]. The behavior of these 'smart' polymers, governed by a combination of electrostatic and hydrophobic interactions, leads to unique properties which can be capitalized upon in a number of applications, including flocculating agents [17–19,28], temperature sensitive coatings [14] or the biomedical field [29–32]. However, a major problem encountered in the study of copolymers prepared by free radical polymerization concerns the heterogeneity in composition of the full conversion samples. In general, the inhomogeneities are due to differences in the reactivity ratios of the monomers that produce a drift in the copolymer composition as the reaction proceeds. An heterogeneous microstructure might have some severe effects on the overall properties of the systems and can even lead in the case of associating water-soluble polymers to phase separation [33]. Over the last years, we have addressed extensively this problem, which is often ignored in the literature. In particular, we showed that polymerization reactions carried out in nanostructured media like micelles or microemulsions, together with an appropriate choice of the components, allows the synthesis of samples with controlled architectures and well defined characteristics [34–36].

In the present study, we have applied free radical microemulsion polymerization process to the synthesis of NIPAM-based ionized polymers. The chemical formulae of the different monomers investigated are reported in Scheme 1. We have synthesized polyelectrolytes and polyampholytes, the latter containing both negative and positive charged units on the same polymer chain. The first part of the paper reports on the application of simple concepts established for the stabilization of emulsions to the formulation of polymerizable microemulsions containing NIPAM and one or two charged monomers of opposite sign. A semi-continuous process was also developed to optimize the

* Corresponding author. Tel.: +33-388-41-40-38; Fax: +33-388-41-40-99.

*E-mail address:* candau@ics.u-strasbg.fr (F. Candau).

0032-3861/01/$ - see front matter 
PII: S0032-3861(01)00445-1

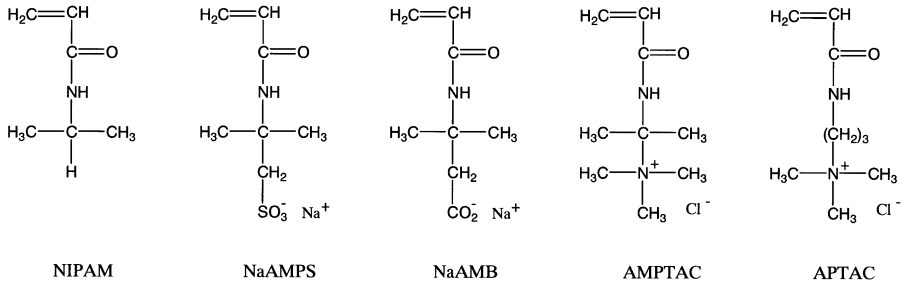


Scheme 1. Monomers employed in the synthesis of polyampholytes.

procedure. To gain more insight into the mechanism of this process, we have followed the particle nucleation with the extent of polymerization by means of dynamic light scattering experiments. The results were compared to the well-established mechanism of batch polymerization in inverse microemulsions. Finally, in the latter part, we investigate the evolution of the composition of samples based on three different monomers (NIPAM, anionic and cationic monomers) with the degree of conversion.

## 2. Experimental section

### 2.1. Materials

*N*-isopropylacrylamide (NIPAM) from Acros was used without further purification. Sodium 2-acrylamido-2-methylpropanesulfonate (NaAMPS) was supplied by CIM Chemicals as a 55 wt% aqueous solution and 2-acrylamido-2-propanetrimethylammonium chloride (APTAC) was obtained from Stockhausen as a 60 wt% aqueous solution. The emulsifier is a blend of polyoxyethylene sorbitan hexaoleate with 50 ethylene oxide residues (HLB = 11.4) and of sorbitan sesquioleate (Montane 83, HLB = 3.7) both provided by SEPPIC. The oil is a narrow-cut isoparaffinic mixture, Isopar M from Exxon, which was filtered before use (boiling range: 207–275°C). Water was a Milli-Q grade. The redox initiator, sodium metabisulfite and cumene hydroperoxide was supplied by Aldrich.

*N*,*N*,2-trimethyl-1,2-propanediamine (DAMP) was a gift from Angus and 3,3-dimethylacrylic acid (DMA, Aldrich) was recrystallized with acetone. The following chemicals obtained from Aldrich were used as supplied: acrylonitrile, acryloyl chloride, methyl iodide, Dowex chloride ion-exchange resin. All these compounds were used for the synthesis of the other monomers (see below).

The microemulsions were prepared by adding with stirring the aqueous monomer solutions in requisite proportions to a mixture of emulsifiers and oil.

### 2.2. Synthesis of monomers

The synthesis of the three following monomers have been reported elsewhere [37–39]. They are briefly described below with some modifications.

1. *NaAMB (sodium 3-acrylamido-3-methylbutanoate)*. Sulphuric acid, 30.4 g (0.31 mol) was added dropwise to a mixture of DMA, 15 g (0.15 mol), acrylonitrile, 7.95 g (0.15 mol) and water, 1.35 g (0.075 mol) cooled to 5°C. *Tert*-butylcatechol was added to avoid polymerization during reaction and workup. The temperature was held at 10–20°C during the sulphuric acid addition and then was allowed to warm at room temperature. After 2 h, the mixture was diluted with 100 ml of water while maintaining the temperature below 40°C. Unreacted DMA precipitated and was separated by filtration. The filtrate was extracted several times with chloroform, which was removed by evaporation. The crude product obtained was recrystallized with a 2-butanone/petroleum ether mixture and gave 9.3 g (36%) of crystals.

$^1$H NMR ($CDCl_3$) $\delta$, 1.49 (6H, s, $CH_3$–C), 2.82 (2H, s, $CH_2$–$CO_2$), 5.63 (1H, dd, acryl), 6.10–6.20 (2H, 2dd, acryl), 6.25 (1H, s, CO–NH).

The sodium salt was obtained by adding the required amount of NaOH in order to get a 50 wt% aqueous solution of NaAMB.

2. *AMPDA (2-acrylamido-2-methylpropanedimethylamine)*. DAMP, 18.0 g (155 mmol) was dissolved in 150 ml of anhydrous THF, and 15.4 g (170 mmol) of acryloyl chloride was added dropwise with stirring. The mixture was held at 10°C by cooling. The product precipitated in the hydrochloride form during the reaction. After 2 h, this precipitate was filtered and washed with THF, and then dissolved in water. The pH of the solution was adjusted to 12 by addition of NaOH. The aqueous phase was then extracted with 2-butanone. The crude product obtained by evaporation was recrystallized with a 2-butanone/petroleum ether mixture (yield: 90%).

$^1$H NMR ($CDCl_3$) $\delta$, 1.40 (6H, s, CH3–C), 2.33 (6H, s, $CH_3$–N), 2.45 (2H, s, N–$CH_2$–C), 5.56 (1H, dd, acryl), 6.08–6.23 (2H, 2dd, acryl), 6.20 (1H, s, CO–NH).

3. *AMPTAC(2-acrylamido-2-methylpropanetrimethylammonium chloride)*. Methyl iodide, 35.9 g (253 mmol) was added to a solution of AMPDA, 4.3 g (25 mmol) in 100 ml of anhydrous ether. The flask was sealed and the reaction was allowed to proceed during two days at room temperature. A white precipitate formed which was determined to be AMPTAI, the quaternized monomer with an iodide counter ion. The product was filtered and washed

with ether. The iodide ion was then exchanged using a Dowex-$Cl^-$ resin to obtain the desired AMPTAC monomer.

Elemental analysis ($C_{10}H_{21}N_2OCl$), calculated: C = 53.9%, H = 9.5%, N = 12.6%, O = 8.5%, Cl = 15.4%, $H_2O$ = 1.1%, Found: C = 53.8%, H = 9.6%, N = 12.5%, O = 8.2%, Cl = 15.9%, I = 0%.

### 2.3. Polymerization procedure

#### 2.3.1. Batch process

The polymerization experiments were carried out in a water-jacketed reaction vessel, after bubbling purified nitrogen through the microemulsion to eliminate oxygen. Then, a solution of cumene hydroperoxide in Isopar M was added, followed by an aqueous solution of sodium metabisulfite drop by drop over 5 min. The redox initiator (0.03 mol% based on monomers) allows a very good control of the beginning of the polymerization. As previously described [40,41], the initial stage of the polymerization is evidenced by the appearance of turbidity and a notable increase of the viscosity of the medium. After a few minutes, the system becomes clear and fluid again, which corresponds to a quantitative yield of polymer.

The polymers were recovered by precipitation in a 2-propanol/acetone mixture, followed by several washings, filtered and dried under vacuum at 45°C. Conversion was determined gravimetrically. In order to eliminate the salt and possible residual impurities, some of the ampholytic polymers were dissolved in an appropriate NaCl aqueous solution and dialyzed against deionized water (membrane Spectra/Por, molecular weight cut off: 15000) before recovering by freeze-drying.

In the case of polymerizations stopped at low conversions, the reaction was stopped at the appropriate point by injection of a cold solution of hydroquinone inhibitor in acetone and precipitation in an excess of a 2-propanol/acetone mixture maintained at 5°C.

#### 2.3.2. Semi-continuous process

In this case, the microemulsion was prepared by mixing only 20% of the overall aqueous phase with the oil and surfactants. The other 80% were placed in a syringe ready to be injected. The microemulsion was purged with nitrogen in order to remove residual oxygen and the initiation of the polymerization was carried out with a simultaneous injection of both components of the redox initiator. Five minutes later, the monomer solution was added dropwise during 1 h. The stirring should be high enough to ensure a good dispersion of the aqueous phase in the polymerizing system. After addition was complete, injection of the initiator was pursued for a further 15 min and stirring was continued for another 1 h. In contrast to the batch process, the system remained totally fluid and optically clear during polymerization and the final state is a slightly bluish transparent microlatex.

The polymers were recovered by the same method as described for the batch process.

### 2.4. Characteristics of copolymers and latexes

#### 2.4.1. Molecular composition

The composition of polymers was determined by elemental analysis. The weight percentages of C, N and H were determined with a Carlo Erba Elemental Analyzer, the sodium content by a gravimetric method (weight of sodium sulfate formed after mineralisation with sulfuric acid) and Cl, O and S by mineralisation using the Schöninger method. The water content in the polymers was measured by Karl–Fisher's method with an automatic KFE452 titrimeter.

#### 2.4.2. Turbidimetry

The optical transmittance of the microlattices was directly measured after polymerization without further dilution in cells of 1 cm thickness using a UV–visible spectrophotometer (Varian DMS 80) operating at a fixed wavelength (600 nm).

#### 2.4.3. Light scattering experiments

The molecular weights of the polymers were determined using an AMTEC SM200 spectrophotometer. The optical source was a helium–neon laser operating at 632.8 nm. Because of the high molecular weight of the polymers, polymer stock solutions were prepared by dissolving the sample at very low concentrations ($\sim 5.10^{-5}$ g $cm^{-3}$) with gentle stirring, 48 h before the measurements.

The solvent used for the experiments was a mixture of methanol/2M NaCl in water (1/1 v/v). Such a solvent mixture was used instead of pure water because it makes it easier to obtain dust-free solutions by centrifugation. As the refractive indexes of both solvents are the same, problems arising from preferential adsorption are suppressed.

The refractive index increments $dn/dC$ were determined on dilute samples ($2 \times 10^{-3} < C < 10^{-2}$ g $cm^{-3}$) in the same solvent mixture with a Brice–Phoenix differential refractometer (wavelength, $\lambda = 632.8$ nm).

#### 2.4.4. Quasi-elastic light scattering experiments

The determination of the size of the latex particles was obtained by means of quasi-elastic light scattering experiments (QELS). The optical source was a spectra physics argon ion laser operating at 488 nm. The time-dependent correlation function of the scattered intensity was derived by using a 288-channel digital correlator. Intensity correlation data were processed by using the method of cumulants [42] to provide the average decay rate, $\langle \Gamma \rangle$ and the variance $v$ of the field autocorrelation function. The latter is a measure of the width of the distribution of the decay rates and is given by:

$$v = \frac{\langle \Gamma \rangle^2 - \langle \Gamma^2 \rangle}{\langle \Gamma \rangle^2}$$

The translational diffusion coefficient $D$ was determined

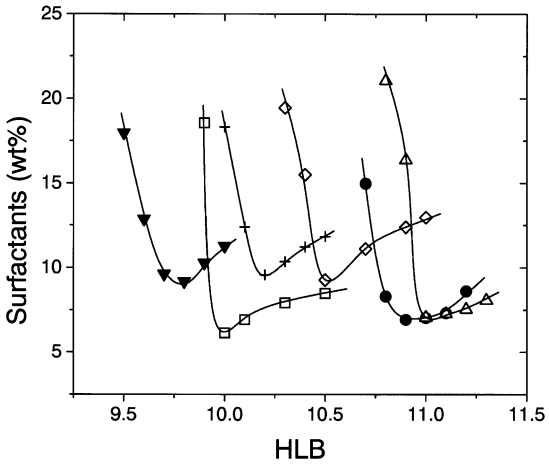


Fig. 1. Percentage of surfactants required for the formation of microemulsions versus HLB for various monomer mixtures and compositions; (▼) NIPAM/NaAMPS 50/50 ($M/W = 0.54$); (□) NIPAM/NaAMPS 20/80 ($M/W = 0.78$); (+) NIPAM/NaAMPS/APTAC 50/40/10 ($M/W = 0.54$); (◇) NIPAM/NaAMPS/APTAC 50/25/25 ($M/W = 0.54$); (●) NIPAM/NaAMPS/APTAC 20/60/20 ($M/W = 0.78$); (Δ) NIPAM/NaAMB/APTAC 20/60/20 ($M/W = 0.78$) ($T = 23$°C).

from $\langle \Gamma \rangle$ according to:

$$\langle \Gamma \rangle = \mathbf{q}^2 D$$

where $\mathbf{q} = 4\pi \sin(\theta/2)/\lambda$ is the scattering vector ($\theta$ the scattering angle, $\lambda$ the wavelength of the incident light in the medium).

The diffusion coefficient $D$ is related in the high-dilution limit to the hydrodynamic radius $R_H$ of the particle according to:

$$R_H = \lim_{\Phi \to 0} \frac{kT}{6\pi\eta_0 D}$$

where $\eta_0$ is the viscosity of the continuous phase.

The microlatices were diluted with pure Isopar M down to a volume fraction of the dispersed phase, $\Phi$, of around 1.5–3.5%. The latter is defined as:

$$\Phi = \frac{V_E + V_M + V_W}{V_{total}}$$

Where $V_E$, $V_M$ and $V_W$ represent the volumes of emulsifiers, monomers and water dispersed in the system, respectively.

## 3. Results and discussion

### 3.1. Formulation

#### 3.1.1. Formulation of microemulsions

First, it must be kept in mind that the formulation of a microemulsion requires more surfactant than a conventional emulsion, because of the need to stabilize a larger overall interfacial area. This drawback can restrict the use of microemulsion polymerization and therefore the first step of the study is to find an inexpensive formulation compatible with an economical process. In previous studies [40,43–46], we have shown that the optimal formulation of monomer-containing microemulsions can be achieved by using the Cohesive Energy Ratio concept (CER) developed by Beerbower and Hill [47] for the stability of classical emulsions. Briefly, the basic assumption of this approach is that the partial solubility parameters of oil ($\delta_O^2$) and emulsifier lipophilic tail ($\delta_L^2$), and of water and hydrophilic head are perfectly matched. When these conditions are met, one gets the following relationship:

$$HLB_o = \frac{20\delta_L^2}{K + \delta_L^2}$$

where $HLB_o$ is the optimum Hydrophile-Lipophile Balance (HLB) of the surfactant when $\delta_L^2 = \delta_O^2$ and $K$ is a constant estimated at 210 for a W/O (water-in-oil) emulsion [47]. It is thus possible to calculate the required HLB for the given oil. This criterion led us to select the following experimental conditions for the microemulsions based on the various monomers listed in Section 2:

Oil: Isopar M ($\delta_O = 7.79$ (cal cm$^{-3}$)$^{1/2}$)
Aqueous phase/oil weight ratio (A/O) = 1
Surfactants: mixture of sorbitan sesquioleate (Montane 83, HLB = 3.7) and of polyoxyethylene sorbitan hexaoleate with 50 ethylene oxide residues (HLB = 11.4). The solubility parameters of the lipophilic tails of these surfactants are equal (same oleate tail, $\delta_L = 7.87$ (cal cm$^{-3}$)$^{1/2}$) indicating complete miscibility. This value is very close to that of the paraffinic oil.

The monomers/water weight ratio, M/W, in the aqueous phase was varied from 0.28 to 1, depending on the amount of NIPAM in the monomer feed.

The complex resulting from the association of the two nonionic surfactants at the W/O interface favors greater stability. In addition, blending surfactants allows the selection of an optimum HLB by varying their composition.

An example of the procedure optimization is given in Fig. 1. It represents the percentage of surfactants required for the formation of a microemulsion as a function of the HLB number, for various types of monomer mixtures and various compositions. The curves delineate the transition between a turbid emulsion and an optically transparent microemulsion. The transition is sharp and can be easily detected by turbidimetry or visual inspection. It can be seen that microemulsions are found in a HLB domain ranging between 9.5 and 11.3. The curves exhibit a minimum, $S_{min}$ for an optimum HLB value, $HLB_{opt}$. Note also the quite low surfactant concentrations needed for the formation of clear systems ($6.1 < S_{min} < 9.6$) in spite of the large proportions of monomers incorporated.

The HLB values are higher than those classically used in inverse emulsion polymerization (HLB = 4–6), and are indicative of microemulsions with a bicontinuous structure, as shown by previous studies performed on other systems

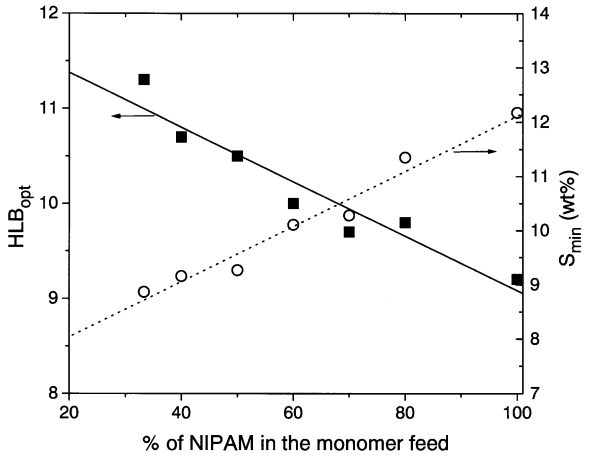


Fig. 2. Variations of $HLB_{opt}$ (■) and $S_{min}$ (○) with the molar content of NIPAM in a NIPAM/NaAMPS/APTAC monomer mixture.

[40,41,43,44]. A bicontinuous structure consists of oily and aqueous domains randomly interconnected over macroscopic distances [48,49]. The formation of microemulsions with a bicontinuous structure can be ascribed to the presence of monomers in large proportions in the systems, which affect the HLB and the interfacial properties. The role of the monomers was thoroughly investigated by our group for other monomer pairs [41,43–45,50–52]. It was found that the water-soluble monomer usually acts as a cosurfactant, leading to a considerable extension of the microemulsion domain in the phase diagram. For example, the cosurfactant role of NaAMPS was confirmed by surface tension experiments [45]. A direct consequence of this effect is an enhancement of the flexibility and fluidity of the interface, which favors the formation of a bicontinuous structure.

The high $HLB_{opt}$ values observed are also partly due to the electrolyte character of the charged monomers [40,50]. Addition of a salting-out type electrolyte like those studied here (NaAMPS, NaAMB, APTAC, AMPTAC) leads to an optimum HLB value larger than that obtained in the absence of salt. The salting-out effect provokes a decrease in the solubility of the ethoxylated surfactants in water. It is therefore necessary to shift the HLB to higher values in order to counterbalance the solubility decrease, for optimum microemulsification. This salting-out effect and its dependence upon the nature of the monomeric salt are shown in Fig. 1. It can be seen that the $HLB_{opt}$ value and the corresponding [$S_{min}$] are little affected by the replacement of NaAMPS by NaAMB, the salting-out effect caused by these two monomers being likely equivalent. The strongest salting-out is indeed observed for the cationic monomer APTAC (compare NIPAM/NaAMPS 20/80 and NIPAM/NaAMPS/APTAC 20/60/20 systems).

### 3.1.2. Effect of the NIPAM content on the formulation

In some experiments carried out on various types of monomer mixtures, we found that an increase of the NIPAM content in the feed tends to decrease the value of the $HLB_{opt}$ and also to increase the minimal amount of surfactants [$S_{min}$] required to stabilize the microemulsion. To confirm this result, we carried out a systematic study on NIPAM/NaAMPS/APTAC mixtures in which the NIPAM concentration was increased from 0.33 (NIPAM/NaAMPS/APTAC 33/33/33) to 1 (100/0/0), those of NaAMPS/APTAC being kept in equimolar proportions. As the NIPAM concentration in water is always kept at 22 wt% (maximum solubility), this amounts to decreasing the overall amount of monomers in the aqueous phase. The variations of the $HLB_{opt}$ and of [$S_{min}$] as a function of the NIPAM molar content in the monomer feeds are reported in Fig. 2. Linear variations are observed in both cases with a decrease in $HLB_{opt}$ and an increase in [$S_{min}$], respectively. The decrease in the $HLB_{opt}$ values can be explained as follows: as the content of ionic monomers decreases upon increasing the NIPAM concentration, the salting-out effect caused by these monomers on the ethylene oxide units of the surfactant becomes less and less pronounced, resulting in the observed decrease in $HLB_{opt}$.

As for the increase of [$S_{min}$], it is directly related to the overall proportions of the monomers in the aqueous phase. As mentioned above, these monomers act as cosurfactants in the formation of microemulsions, which causes a considerable extension of the microemulsion region in the phase diagram. Consequently, if the overall amount of the monomers in the aqueous phase is decreased (see above), one expects more surfactant to be needed to stabilize the microemulsion. This is indeed what is observed in Fig. 2.

## 3.2. Polymerization

### 3.2.1. Stability of the microlatex

In general, the polymerization of bicontinuous microemulsions prepared under the optimal conditions defined above led to stable and transparent microlatex. As a matter of fact, our previous studies performed on other monomer pairs have shown that the interplay between the composition of the initial microemulsion and the stability of the final microlatex is rather subtle, due to the great number of degrees of freedom involved in the formulation [40,41]. This conclusion was based on the following considerations:

(1) In all the cases investigated, the stability, fluidity and transparency of the initial microemulsion was not maintained in the course of the reaction. At the early stages of the reaction, the system became turbid and the viscosity of the medium increased. The end of the polymerization was characterized by a return to clarity and fluidity. These changes were found to be related to the progressive evolution of the bicontinuous structure towards a globular configuration, as was shown from QELS experiments [40,41 and below]. This result can be qualitatively understood by the consumption of the portion of monomers located at the W/O interface. This induces a change in the composition of the interfacial film and of the film curvature energy, resulting in the destabilization of the bicontinuous microemulsion, with

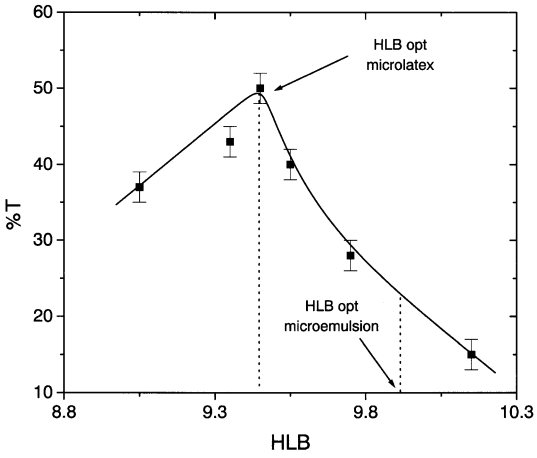


Fig. 3. Optical transmittance of NIPAM/NaAMPS 50/50 microlatexes versus HLB (thickness of the cell: 1 cm).

a possible shift in the phase diagram. The globular configuration reached at the end of the reaction corresponds to the minimum free energy of the system.

(2) On the other hand, when ionic monomers are polymerized in microemulsions, it was found that is not necessary to start with a transparent microemulsion to get a clear and stable latex [40,41]. In this case, the turbidity observed for some systems was not caused by the existence of a polyphasic domain arising from insufficient amounts of surfactant but rather to the high electrolyte content which lowered the cloud point of the surfactants (salting-out). In the course of polymerization, the monomers located partially at the interface diffuse into the particles and the salt-saturated aqueous phase becomes progressively used up, accounting for the clarity of the systems at the end of the reaction.

Based on the above considerations, Candau and Anquetil were able to define the stability domains for microemulsions based on AM-NaAMPS monomers and for the corresponding microlatex [40]. However, no optimum related to the microlatex stability could be quantified. This led us to investigate in more details the correlation between optimum microemulsification (prior to polymerization) and the stability of the latex (after polymerization). In particular, we have examined the effect of HLB and of the surfactant content on the microlatex stability. The system selected was a microemulsion based on NIPAM/NaAMPS (50/50) as the monomer feed.

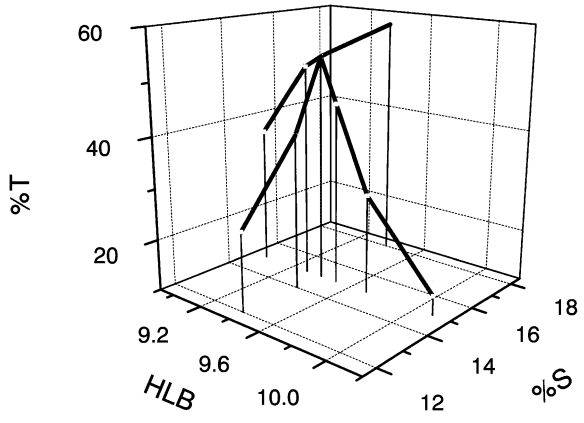


Fig. 4. Optical transmittance versus HLB and surfactant concentration for NIPAM/NaAMPS 50/50 microlatexes (thickness of the cell: 1 cm).

In a first step, the HLB of the surfactant mixture was varied in the vicinity of the optimum HLB value ($HLB_{opt}$) from 9.0 to 10.1, while the amount of surfactant was kept constant at 15 wt%. The results can be seen in Fig. 3 where the optical transmittance of the microlatex as a function of the surfactant HLB is reported. One observes a shift of the $HLB_{opt}$ going from 9.9 for the initial microemulsion (prior to polymerization) to 9.4 for the microlatex (after polymerization). This HLB shift likely corresponds to the incorporation of the ionic monomers in the copolymer. It should also be noted that for systems with HLB values $\leq$9.4, the initial microemulsions were opaque.

In a second step, we have varied the amount of surfactant mixture from 12 to 18 wt% keeping fixed the HLB of the microemulsion at the optimum value defined above for the microlatex ($HLB_{opt} = 9.4$). The results taken together allowed us to draw the three dimensional diagram shown in Fig. 4. The shape of the diagram is indeed what could be foreseen; an increase in surfactant content tends to increase the optical transparency of the microlatex (smaller size of the particles). It is worthwhile to note however that the latex prepared at HLB = 9.4 and 12 wt% of surfactants has an optical transmittance higher than the one prepared at a HLB = 9.9 (optimum for the initial microemulsion) and 15 wt% of surfactants.

### 3.2.2. Optimization of the procedure

*Increase of the aqueous-to-oil phase ratio in the batch process*. In order to increase the solid contents in the final products, we have carried out a series of polymerizations in which the monomer aqueous phase to oil phase weight ratio (A/O) was varied and equal to 60/40, 65/35, 70/30 and 75/25, respectively. The other parameters were kept constant (monomers to water weight ratio: 0.78 and surfactant level: 14 wt%). The monomers feed investigated was NIPAM/NaAMPS/APTAC 20/60/20. The latex obtained with A/O = 60/40 was clear and fluid, indicating that the bicontinuous structure of the microemulsion was still maintained for this ratio. This allows one to improve the solid content from 18.8 wt% (A/O = 50/50) to 22.6 wt%. Beyond this limit, a translucent gel (65/35) or very viscous latex were obtained which suggest that the initial microemulsion was no longer bicontinuous but rather of O/W type.

*Semi-continuous polymerization*. The semi-continuous process, currently used in direct emulsion polymerization, presents a number of advantages over the batch process; it offers a way to increase the solids content and also it can correct for the drift in copolymer composition when monomers of different reactivity ratios are used. However, such a

Table 1
Characteristics of NIPAM/NaAMPS/APTAC 20/60/20 latexes prepared by semi-continuous (S.C.) and batch polymerization

| Latex | | Isopar $M$ (wt%) | Aq. phase (wt%) | $S$ (wt%) | $M$ (wt%) | $\Phi$ (vol%) | $M/S$ (g/g) | $R_H$ (nm) | $v$ (%) | $M_W$ ($10^6$) |
|---|---|---|---|---|---|---|---|---|---|---|
| S.C. | 20% | 67.9 | 13.6 | 18.5 | 5.9 | 24.5 | 0.32 | 27.5 | 10.0 | 2.6 |
| S.C. | 40% | 59.8 | 23.9 | 16.3 | 10.4 | 31.4 | 0.64 | 24.1 | 11.6 | 2.2 |
| S.C. | 60% | 53.4 | 32.0 | 14.6 | 14.0 | 37.1 | 0.96 | 32.4 | 16.8 | 1.0 |
| S.C. | 80% | 48.2 | 38.6 | 13.2 | 16.9 | 42.0 | 1.28 | 39.7 | 8.8 | 1.2 |
| S.C. | 100% | 44.0 | 44.0 | 12.0 | 19.2 | 46.2 | 1.60 | 34.3 | 5.3 | 1.1 |
| Batch | 100% | 44.0 | 44.0 | 12.0 | 19.2 | 46.2 | 1.60 | 42.9 | 5.7 | 4.3 |

process cannot be employed in conventional inverse emulsion polymerization, due to the difficulty of achieving adequate shear in the reactor while still maintaining a stable dispersion. In the present case, the use of a semi-continuous process for the polymerization of water-soluble monomers should be possible since the starting microemulsions are thermodynamically stable. The semi-continuous polymerization of hydrophobic monomers in direct microemulsions was recently described by several groups [53–55] but to the best of our knowledge the present study is the first example of the use of a semi-continuous polymerization in inverse systems. An example of the procedure used is detailed in the Experimental Section. The advantages of the process are twofold:

(1) It allows one to significantly decrease the surfactant content required to stabilize the final microlatex since, for a system based on NIPAM/NaAMPS/APTAC 20/60/20, it is reduced from 14 wt% (batch process) to 8 wt% (solid content: 20.1 wt% in both cases).

(2) It allows the stability, clarity and fluidity of the system to be maintained during the whole polymerization reaction due to the fact that one starts now with a microemulsion which is no longer bicontinuous (as in batch process) but more likely globular owing to the low aqueous phase/oil ratio (0.2 compared to 1 in the batch process). In this case, one does not expect any structural change of the systems as seen in the batch process. Indeed, no change in appearance is observed except for a bluish appearance of the dispersions.

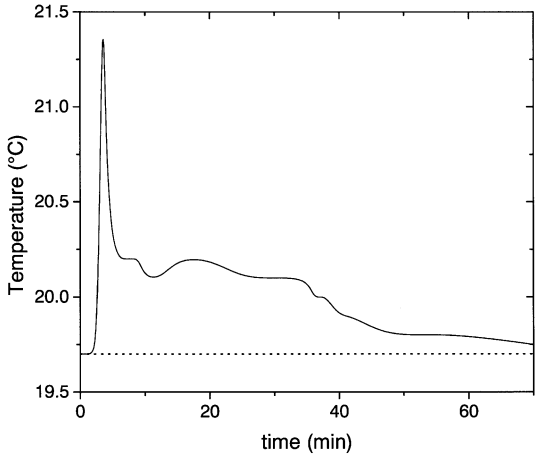


Fig. 5. Temperature changes in the reaction medium during a semi-continuous polymerization (60% sample).

### 3.3. Polymerization mechanism in the semi-continuous process

Before turning to the semi-continuous process, we recall below the mechanism of batch polymerization in globular W/O microemulsions [50,56,57]. The two main features are the following:

(1) The particle size of the final microlatex ($d \sim$ 20–40 nm) is always larger than that of the initial monomer-swollen micelle. Nucleated particles grow by addition of monomer from other inactive micelles, either by coalescence with neighboring micelles or by monomer diffusion through the continuous phase.

(2) The average number of polymer chains contained in each particle is very low, one in the limiting case. This is in striking contrast with latexes prepared in inverse emulsion where this number can reach several thousands. In microemulsions, the level of emulsifier is greatly augmented with respect to that in emulsions and the monomer concentration is usually lower. Therefore and as a result of the particle growth, small micelles of uniform size are always in excess throughout the reaction mixture. Their high total interfacial area compared to that of the nucleated polymer particles implies that the micelles preferentially capture primary radicals generated in the continuous phase. This leads to a process of continuous particle nucleation with each particle formed in one step; again this is in contrast with what is observed in conventional emulsion polymerization where the first nucleation stage (Interval I) is followed by a particle growth, sometimes at constant particle number (Interval II).

The above mechanistic scheme is now well established for batch polymerization reactions but the features of the semi-continuous polymerization are still unknown. In order to gain more insight into the mechanism and particle nucleation of this process, we have followed the particle size evolution as a function of the extent of polymerization by QELS experiments. For this purpose, we have performed five experiments on NIPAM/NaAMPS/APATC 20/60/20 systems stopped at different reaction times, corresponding to a partial addition of the aqueous phase in the reactor equal to 20, 40, 60, 80 and 100 wt%, respectively, where 100% corresponds to an aqueous phase/oil ratio of 1. Table 1

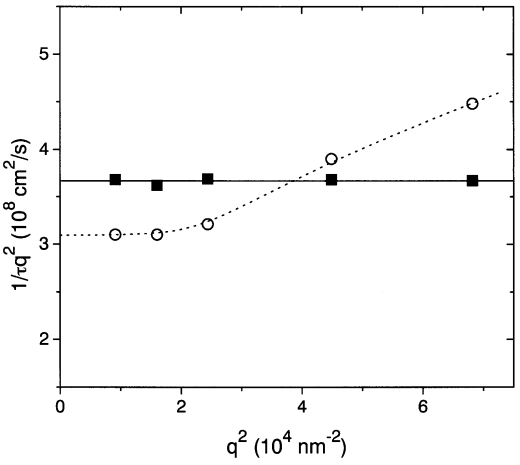


Fig. 6. Variation of $1/\tau q^2$ vs. $q^2$ for NIPAM/NaAMPS/APTAC 20/60/20 latex obtained after addition of 20wt% (■) and 60 wt% (○) of the aqueous phase.

summarizes the compositions of the systems, investigated together with the volume fractions of the dispersed phase. Note that the first experiment (20% of aqueous phase) is equivalent to a batch process, since there is no further addition of the aqueous phase. In all cases, the inverse microlatexes formed are perfectly transparent and stable.

As the polymerization reaction is quite exothermic, we have also followed the temperature changes during the reaction. A typical curve for the changes in temperature during polymerization is shown in Fig. 5; it corresponds to an experiment stopped after addition of 60% of the aqueous phase. The sharp rise observed during the first few minutes corresponds to the 20% batch polymerization. Then, upon slow addition of the remaining aqueous phase (semi-continuous process), a second stage is reached, characterized by a slight exothermicity, which lasts until the end of monomer addition.

The light scattering data have been analyzed using the cumulants method that provides a correlation time, $\tau(\tau = 1/\langle\Gamma\rangle)$, and a variance, $v$, which gives an estimate of the particle polydispersity. The variation of $1/\tau\mathbf{q}^2$ vs. $\mathbf{q}^2$ is reported in Fig. 6 for two samples. It is seen that $1/\tau\mathbf{q}^2$ is independent of $\mathbf{q}^2$ for the 20% sample, whereas one observes an increase of $1/\tau\mathbf{q}^2$ with $\mathbf{q}^2$ for the 60% sample. The latter behavior is an indication of significant polydispersity of the system. This is confirmed by the value of the variance, which is of the order of 0.17. The translational diffusion coefficient $D$ is obtained from the extrapolation of $1/\tau\mathbf{q}^2$ to $\mathbf{q} \rightarrow 0$. For all the samples investigated, $D$ is found to be independent of the volume fraction $\Phi$ of the dispersed phase. This indicates that the microlatexes behave as hard spheres without strong interactions between the particles. From this value of $D$, one deduces the average hydrodynamic radius, $R_H$. The $R_H$ values and the corresponding variances are reported in Table 1. The values of $R_H$ and $v$ go roughly through a maximum for the 80 and 60% systems, respectively.

A more detailed analysis of the light scattering data based on the Laplace transform method provides additional

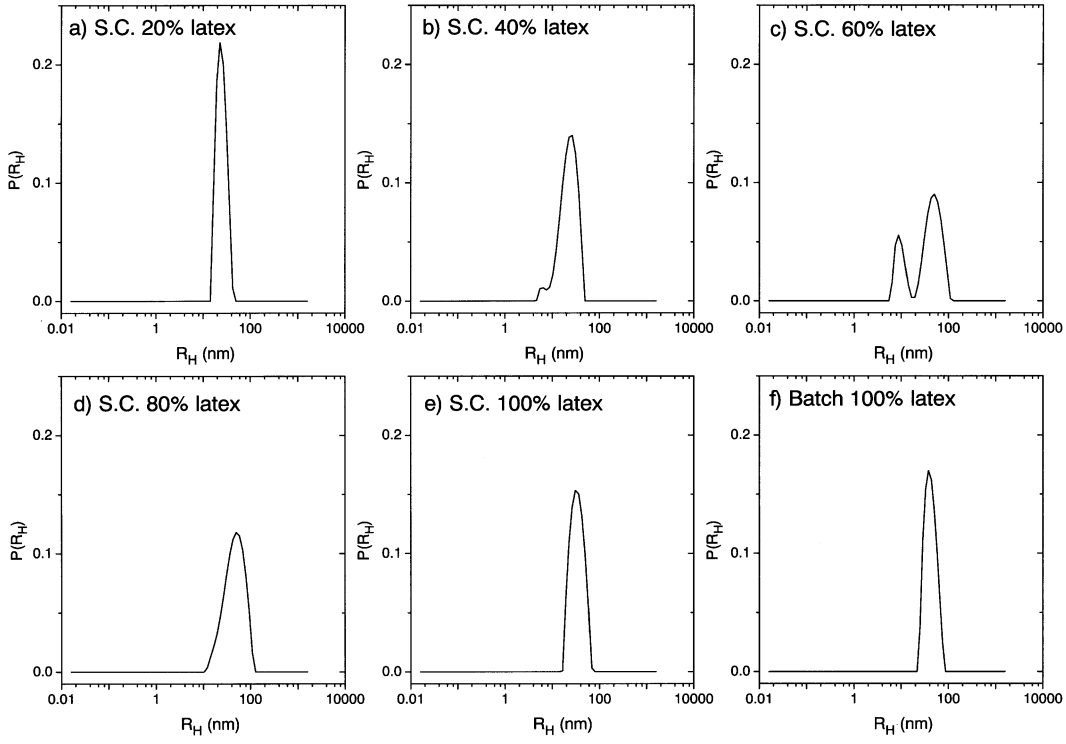


Fig. 7. Distribution function $P(R_H)$ of the particle sizes for NIPAM/NaAMPS/APTAC 20/60/20 latexes stopped after addition of various amounts of the aqueous phase; (a)–(e): semi-continuous process; (f): batch process.

information on the particle size distribution. Fig. 7 shows the development of the particle size distribution at a given volume fraction ($\Phi = 3.5\%$) and a given angle ($\theta = 40°$) with the extent of reaction. The 20% initial latex has a well characterized mean size distribution. In the course of polymerization, a second population of smaller particles is nucleated (40% latex), which increases with time to form a bimodal distribution for the 60% latex, accounting thus for the large increase in polydispersity measured (see Table 1). As the reaction proceeds, the smaller population disappears at the expense of the bigger one, with a progressive narrowing of the peak (80% latex) to finally obtain after 100% addition of the aqueous phase a microlatex with a low polydispersity and an average radius of 34.3 nm, that is about 20% larger than the initial 20% latex. This value (100% semi-continuous) is to be compared with $R_H \sim 43$ nm obtained for a similar latex but prepared in batch (Table 1). In both cases, the distribution curves are comparable with close values of the width (Fig. 7e and f).

To understand the above results, one has to keep in mind that the equilibrium swelling of a latex particle in the presence of solvent results from two opposing effects: the osmotic contribution (which tends to swell the particle) is counterbalanced by the interfacial free energy between the latex particle and the solvent (which tends to shrink it).

In a previous study, carried out on a batch polymerization of a globular W/O microemulsion, it was found that particle size increased with increasing monomer/surfactant weight ratio (M/S) [58]. This result is directly linked to the increase in interfacial area, which occurs upon increasing this ratio. The same trend is also observed in the present study since the hydrodynamic radius measured for the 20% latex ($R_H = 27.5$ nm) is significantly smaller than that of the 100% batch latex ($R_H = 42.9$ nm). However, in the semi-continuous process, one observes an interesting effect, namely the occurrence of a second population of smaller particles for intermediate M/S ratios (Fig. 7b and c). This can be understood by considering that a very large number of small surfactant micelles still coexist with the latex particles in the 20% system when the monomer aqueous phase and initiator are added in the reactor. Then, the polymerization rate is so fast that the system is always under monomer-starved conditions. So, even though the thermodynamic equilibrium favors the diffusion of monomers within the latex particles (Kelvin equation) the latter process is slow compared to the micellar nucleation. Furthermore, it can be assumed that when a system contains several monomers, the diffusion in the particles is reduced [59,60]. Still, owing to the competition between the micellar nucleation and the diffusion process, one observes simultaneously the formation of new particles and the growth of the pre-formed particles. This competition reveals itself particularly for the 60% latex in which the two particle classes have about the same weight. Upon further increasing the volume fraction of the dispersed aqueous phase, (80% system), the small particles tend to disappear. In fact, as the particle density increases, the particle swelling becomes predominant at the expense of the nucleation of new micelles swollen by monomer. In addition, the particle size reaches an upper critical value resulting from the equilibrium between the osmotic swelling and the interfacial free energy. For the 100% latex, all the particles have swollen up to their critical size and one obtains a system with a rather low polydispersity ($v = 5\%$).

For a meaningful comparison between the batch and the semi-continuous processes, the above experiments were performed with 12 wt% of surfactants. As the latter process allows the use of a lesser amount of surfactant, an experiment was also carried out in semi-continuous with 8 wt% of surfactant and 100% of the aqueous phase. The average hydrodynamic radius was found to be 37.5 nm, a value close to that measured with 12 wt% of surfactant ($R_H = 34.3$ nm). An advantage of this semi-continuous process is that the high number of micelles still present in the microlatex after polymerization can be used to stabilize additional aqueous phase without increasing drastically the size of the particles.

### 3.4. Copolymer characteristics

#### 3.4.1. Molecular weights

The average molecular weights of the polymers have been determined by light scattering. As expected for batch polymerization reactions in heterogeneous media [50], the values are high and range between $4 \times 10^6$ and $9 \times 10^6$, depending on the experimental conditions.

The molecular weights of the samples prepared in semi-batch are significantly smaller than those in batch (see Table 1). This result is classically observed for polymerizations carried out under monomer-starved conditions and results from the low value of the monomer concentration in the particles compared to that of the polymer (usually $>0.80$) [61]. Thus, the molecular weight drops from $2.6 \times 10^6$ (20% latex, seed stage) to a roughly constant value around $1.1 \times 10^6$ at the late stages of the reaction.

Note also the difference in molecular weights between the 20 and 100% samples, both carried out in batch. This can be explained by the different overall monomer concentrations in the medium; the higher [M], the greater $M_W$ [62].

#### 3.4.2. Compositional analysis of the samples

The composition of the copolymers can be determined from the sulphur, nitrogen, chlorine and sodium contents obtained by elemental analysis. As the charged units of polyampholytes may pair with their inorganic counterions or with the oppositely charged mer units with a loss of NaCl, different species should be distinguished (see Scheme 2). AMPS and APTA represent, respectively, a NaAMPS unit without $Na^+$ and a APTAC unit without $Cl^-$, owing to ion-pair formation (AMPS–APTA). It should be noted that the following calculation applies for both APTAC and AMPTAC cationic monomers (described here for APTAC).

The number of the different units contained in 100 g of

Table 2
Copolymer compositions calculated from elemental analysis data

| Monomer feed composition (mol%) | | | Polymer composition (mol%) | | |
|---|---|---|---|---|---|
| NIPAM | NaAMPS | APTAC | NIPAM | NaAMPS | APTAC |
| 20 | 60 | 20 | 22.1 | 56.1 | 21.8 |
| 80 | 10 | 10 | 80.3 | 10.1 | 9.6 |
| 50 | 25 | 25 | 46.2 | 26.8 | 27.0 |
| NIPAM | NaAMPS | AMPTAC | NIPAM | NaAMPS | AMPTAC |
| 50 | 25 | 25 | 47.3 | 25.6 | 27.1 |

samples can be calculated as follows:

Number of NaAMPS and AMPS units: $n$(NaAMPS + AMPS) = %S/32
Number of NaAMPS units: $n$(NaAMPS) = %Na/23
Number of AMPS units: $n$(AMPS) = $n$(NaAMPS + AMPS) − $n$(NaAMPS)
Number of APTA units: $n$(APTA) = $n$(AMPS)
Number of APTAC units: $n$(APTAC) = %Cl/35.5
Number of APTAC and APTA units: $n$(APTAC + APTA) = $n$(APTAC) + $n$(APTA)
Number of NIPAM units: $n$(NIPAM) = %N/14 − {$n$(NaAMPS + AMPS) + 2$n$(APTAC + APTA)}

The molar percentages of the different monomers in the terpolymer can be deduced from the above data. The values of several terpolymers of variable compositions are reported in Table 2 and compared to the initial monomer feeds. Good agreement is observed between both sets of values. It should be noted that dialyzed and non-dialyzed samples have the same compositions, indicating that the purification of the polymer by several washings is efficient. Ampholytic polymers were nevertheless dialyzed in order to remove the residual salt.

### *3.4.3. Evolution of the composition with the degree of conversion*

The determination of the *co*- or *ter*-polymer composition at full conversion provides only a mean value of the overall composition. As the solution properties of copolymers are in general very sensitive to the heterogeneity in composition, it was important to evaluate the latter parameter for the systems investigated here. This determination is particularly relevant for polyampholytes since previous experimental and theoretical studies have shown that their conformation and properties were directly related to their monomer sequence distribution [63–65]. In the case of microemulsion polymerization, it was found that this process tends to improve the structural homogeneity of fully charged polyampholytes with values of reactivity ratios close to unity [36]. This result was accounted for by the marked differences between the microemulsion process and others, in terms of microenvironment (charge screening and preferential orientation of the monomers at the W/O interface) and mechanism (interparticle collisions with complete mixing). The case of ampholytic terpolymers is more complex. A microstructure study of ampholytic terpolymers prepared by microemulsion polymerization and based on acrylamide (AM) as a neutral monomer, NaAMPS and 2-methacryloyloxyethyltrimethylammonium chloride (MADQUAT) as charged monomers, revealed a rather significant drift in terpolymer composition, the monomer reactivities depending on the ionic strength, i.e. on the monomer feed composition [66]. The latter point might be related to the fact that these three monomers contained a different polymerizable group. On the contrary, the monomers investigated for the present purpose, i.e. NIPAM, NaAMPS, APTAC, bear almost an identical polymerizable function.

The variation in copolymer composition with the degree of conversion has been determined for the three following

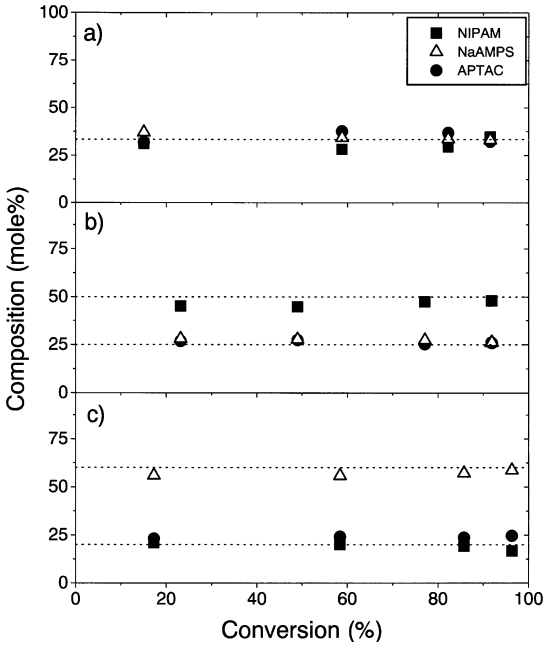


Fig. 8. Terpolymer compositions versus conversion for NIPAM/NaAMPS/APTAC systems (data points) with different monomer feed compositions (dotted lines): (a) NIPAM/NaAMPS/APTAC 33.3/33.3/33.3, (b) NIPAM/NaAMPS/APTAC 50/25/25, (c) NIPAM/NaAMPS/APTAC 20/60/20.

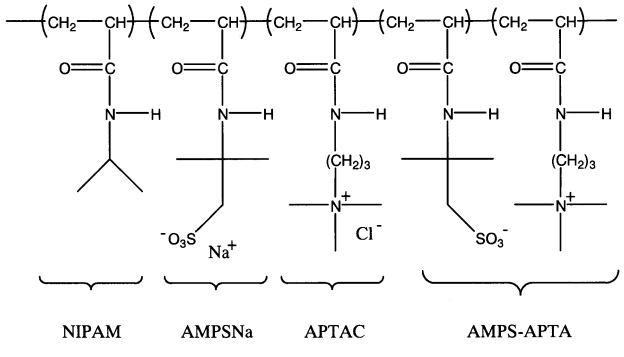


Scheme 2. Structure of a polyampholyte.

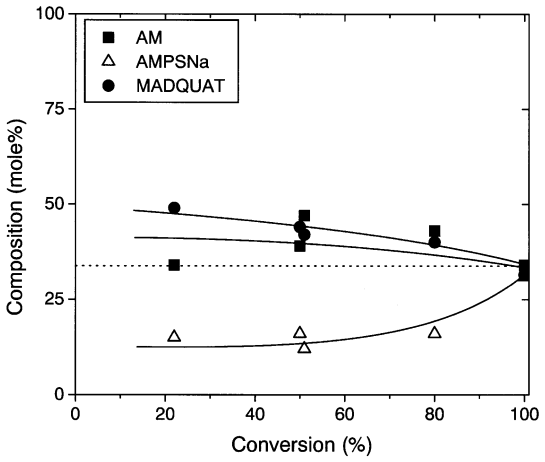


Fig. 9. Terpolymer composition versus conversion for a AM/NaAMPS/MADQUAT system with a monomer feed composition of 33.3/33.3/33.3, respectively (dotted line). (from Ref. [66]).

initial monomer feeds: NIPAM/NaAMPS/APTAC: 50/25/25; 20/60/20; 33.3/33.3/33.3. The average copolymer composition-conversion data are reported in Fig. 8. In all cases, the copolymer composition values determined at various degrees of conversion are close to that of the monomer feed (dotted lines), within the experimental errors of the elemental analysis. This strongly suggests that the terpolymers are homogeneous in composition. For comparison, in Fig. 9 the data obtained by S. Neyret et al. are reported for a terpolymer of the same monomer feed composition as in Fig. 8a, also prepared by microemulsion polymerization but based on AM/NaAMPS/MADQUAT [66]. A significant drift in composition is observed, in striking contrast with the present data, confirming that the choice of monomers is of prior importance in terpolymerization reactions, regardless of the type of process used.

## 4. Conclusion

The aim of the present study was to extend the microemulsion polymerization process previously developed for conventional water-soluble polymers to the synthesis of stimuli-responsive polymers, namely NIPAM-based polyelectrolytes and polyampholytes. In a first step, we have analyzed the general criteria required to achieve an optimal formulation of the polymerizable microemulsions. Particular attention was directed toward the role of the various monomers investigated: their HLB and their possible effects as cosurfactants and/or electrolytes on the W/O interfaces and the resulting phase equilibria. As cosurfactants, they increase the fluidity and flexibility of the interface, which favors the formation of a bicontinuous structure; as electrolytes, they induce the latter structure. These characteristics result in a much higher value of the optimum HLB than that required in conventional inverse emulsions. Taking into account the different parameters in the formulation, we could correlate the optimum microemulsification (prior to polymerization) to the stability of the microlatex (after polymerization).

The final products consist of stable and clear microlatexes of small particle size containing up to 20 wt% of high-molecular weight polymers in the medium. However, a general drawback of the process lies in the high surfactant to monomer ratio usually employed in the initial microemulsions [50]. To overcome this problem, we have developed a semi-continuous process, which allowed us to decrease the surfactant content required to stabilize the final microlatex by more than 40%, while still maintaining the stability and clarity of the microlatex. To our knowledge, this is the first example of the use of a semi-continuous polymerization in inverse (i.e. water-in-oil) systems.

A dynamic light scattering study on the particle nucleation occurring in the semi-continuous process indicates that the systems are maintained under monomer-starved conditions throughout the reaction. After completion, the latex reaches a critical size ($d \sim 70$ nm) which is the result of the equilibrium between osmotic swelling and the interfacial free energy.

The use of microemulsion polymerization combined with an appropriate choice of the various monomers involved — they bear the same polymerizable group — leads to copolymers which are homogeneous in composition, as attested by the evolution of the composition with conversion.

Such well defined copolymers are therefore good candidates for physical studies and their properties in aqueous solution will be the subject of a forthcoming paper.

## Acknowledgements

The authors wish to thank P. Mallo, G. Tabacchi and J.P. Boiteux (SEPPIC) for stimulating discussions and their continued interest in this work. They are grateful to M. Duval (ICS) for his help in the QELS experiments and to K. Landfester (MPIKG, Golm) for her comments on the particle nucleation mechanism. Financial support by SEPPIC is gratefully acknowledged.

## References

[1] Bae YH, Okano T, Kim SW. J Control Release 1989;9:271.
[2] Tanaka T. Polymer 1979;20:1404.
[3] Kopecek J, Vacik J, Lim D. J Polym Sci, Part A1: Polym Chem 1971;9:2801.
[4] Park K, Robinson JR. J Control Release 1985;2:47.
[5] Suzuki A. Adv Polym Sci 1993;110:201.
[6] Eisenberg SR, Grodzinski AJ. J Membr Sci 1984;19:173.
[7] Kwon I, Bae YH, Okano T, Kim SW. Nature 1991;354:291.
[8] Glass JE, editor. Advances in chemistry series, vol. 223. Washington, DC: American Chemical Society, 1989.
[9] Schulz DN, Glass JE, editors. ACS Symposium Series, vol. 462. Washington DC: American Chemical Society, 1991.
[10] Heskins M, Guillet JE. J Macromol Sci, Chem 1968;A2:1441.
[11] Chiklis CK, Grasshoff JM. J Polym Sci, Part A2: Polym Phys 1970;8:1617.

[12] Fujishige S, Kubota K, Ando I. J Phys Chem 1989;93:3311.
[13] Winnik FM. Macromolecules 1990;23:233.
[14] Schild HG. Prog Polym Sci 1992;17:163.
[15] Winnik FM, Ottaviani MF, Bossmann SH, Pan WS, Garciagaribay M, Turro NJ. Macromolecules 1993;26:4577.
[16] Vesterinen E, Tenhu H, Dobrodumov A. Polymer 1994;35:4852.
[17] Deng Y, Pelton R. Macromolecules 1995;28:4617.
[18] Wu C, Zhou S. Macromolecules 1995;28:8381.
[19] Aoki T, Nagao Y, Sanui K, Ogata N, Kikuchi A, Sakurai Y, Kataoka K, Okano T. Polym J 1996;28:371.
[20] Jones MS. Eur Polym J 1999;35:795.
[21] Chen G, Hoffman AS. Nature 1995;373:49.
[22] Chen G, Hoffman AS. Macromol Rapid Commun 1995;16:175.
[23] Yoo MK, Sung YK, Cho CS, Lee YM. Polymer 1997;38:2759.
[24] Tao L, Vesterinen E, Tenhu H. Polymer 1998;39:641.
[25] Durand A, Hourdet D. Polymer 1999;40:4941.
[26] Durand A, Hourdet D. Polymer 2000;41:545.
[27] Durand A, Hourdet D. Macromol Chem Phys 2000;201:858.
[28] Snowden MJ, Vincent B, Morgan JC. GB Patent, 2262117A, 1993.
[29] Brazel CS, Peppas NA. Macromolecules 1995;28:8016.
[30] Snowden MJ, Thomas D, Vincent B. Analyst 1993;118:1367.
[31] Chen G, Hoffman AS. Bioconj Chem 1993;4:509.
[32] Bae YH, Okano T, Kim SW. Makromol Chem, Rapid Commun 1988;9:185.
[33] Jiménez Regalado E, Selb J, Candau F. Macromolecules 2000;33: 8720.
[34] Candau F, Zekhnini Z, Heatley F. Macromolecules 1986;19:1895.
[35] Volpert E, Selb J, Candau F. Macromolecules 1996;29:1452.
[36] Corpart JM, Selb J, Candau F. Polymer 1993;34:3873.
[37] Hoke D, Robins R. J Polym Sci, Polym Chem Ed 1972;10:3311.
[38] McCormick CL, Blackmon KP. Polymer 1986;27:1971.
[39] Kathmann EE, Salazar LC, McCormick CL. Polym Prepr (Am Chem Soc, Div Polym Chem) 1991;32(1):98.
[40] Candau F, Anquetil JY. In: Shah DO, editor. Micelles, microemulsions, and monolayers. New York: Marcel Dekker, 1998. p. 193–213, chapter 8.
[41] Candau F, Zekhnini Z, Durand JP. J Colloid Interface Sci 1986;114:398.
[42] Cummins HZ, editor. Photon correlation and light beating spectroscopy. New York: Plenum Press, 1974.
[43] Holtzscherer C, Candau F. Colloids Surf 1988;29:411.
[44] Buchert P, Candau F. J Colloid Interface Sci 1990;136:527.
[45] Corpart JM, Candau F. Colloid Polym Sci 1993;271:1055.
[46] Candau F. In: Mittal KL, Kumar P, editors. Handbook of microemulsion science and technology. New York: Marcel Dekker, 1999. p. 679–712, chapter 22.
[47] Beerbower A, Hill MW. McCutcheon's detergents and emulsifier annual. Ridgewood, NJ: Allured Publish Corporation, 1971. p. 223–35.
[48] Scriven LE. Nature (Lond) 1976;263:123.
[49] Friberg S, Lapczynska I, Gillberg G. J Colloid Interface Sci 1976;56:19.
[50] Candau F. Polymerization in organized media. Philadelphia. In: Paleos CM, editor. New York: Gordon and Breach Science, 1992. p. 215–82, chapter 4.
[51] Holtzscherer C, Candau F. J Colloid Interface Sci 1988;125:97.
[52] Candau F. Polymer association structures: microemulsions and liquid crystals. El-Nokaly M, editor. ACS Symposium Series 1989;384:47–61, chapter 4.
[53] Ming W, Jones FN, Fu S. Macromol Chem Phys 1998;199:1075.
[54] Roy S, Devi S. Polymer 1997;38:3325.
[55] Ming W, Jones FN, Fu S. Polym Bull 1998;40:749.
[56] Candau F, Leong YS, Pouyet G, Candau SJ. J Colloid Interface Sci 1984;101:167.
[57] Candau F, Leong YS, Fitch RM. J Polym Sci, Polym Chem Ed 1985;23:193.
[58] Candau F, Buchert P. Colloids Surf 1990;48:107.
[59] Torza S, Mason SG. J Colloid Interface Sci 1970;33:67.
[60] Webster AJ, Cates ME. Langmuir 1998;14:2068.
[61] Lovell PA. In: Lovell PA, El-Aasser MS, editors. Emulsion polymerization and emulsion polymer. Chichester: Wiley, 1997. p. 239–75, chapter 7.
[62] Holtzscherer C, Durand JP, Candau F. Colloid Polym Sci 1987;265: 1067.
[63] Candau F, Joanny JF. In: Salamone JC, editor. Polymeric materials encyclopedia, vol. 7. Boca Raton: CRC Press, 1996. p. 5476–88.
[64] Wittmer J, Johner A, Joanny JF. Europhys Lett 1993;24:263.
[65] Neyret S, Baudouin A, Corpart JM, Candau F. In: Mallamace F, editor. Scaling concepts and complex fluids, vol. 16. Il Nuovo Cimento, 1995. p. 669–74.
[66] Neyret S, Candau F, Selb J. Acta Polym 1996;47:323.